

BEAM DIAGNOSTICS FOR NEW BEAM TRANSPORT LINE OF PF-AR

R. Takai*, T. Honda, T. Obina, M. Tadano, H. Sagehashi,
 KEK Accelerator Laboratory and SOKENDAI, 1-1 Oho, Tsukuba, Ibaraki, Japan

Abstract

The beam transport line (BT) for the Photon Factory Advanced Ring (PF-AR), which is a 6.5-GeV light source of KEK, has been recently renewed. The new BT dedicated to PF-AR allows not only simultaneous operation with the SuperKEKB storage ring, which has a much shorter Touschek lifetime, but also the top-up operation via 6.5-GeV full-energy injection. The construction, including tunnel excavation, was completed by the end of 2016, and the commissioning was performed for one month from February 2017. Standard beam monitors, such as stripline beam position monitors, screen monitors, beam loss monitors, and fast current transformers are installed in the new BT and contribute greatly to accomplishing the commissioning in a short period of time. This paper discusses details of these monitors and some commissioning results obtained by using them.

INTRODUCTION

The Photon Factory Advanced Ring (PF-AR), which is a 6.5-GeV electron storage ring of KEK, is a dedicated light source for generating pulsed hard X-rays. The beam transport line (BT) for injecting electron beams to PF-AR has been renewed recently [1]. Before the renewal, the continuous injection for KEKB, which is an electron-positron collider of KEK, had to be interrupted for about 15 min at each injection for PF-AR, because a part of the BT was shared with it. Following the upgrade of KEKB to SuperKEKB, the Touschek lifetime is shortened to ~10 min [2]; therefore, such interruptions should be avoided. This is the main reason why the dedicated BT for PF-AR was constructed. The principal parameters of PF-AR are listed in Table 1.

Table 1: Principal Parameters of PF-AR

Beam Energy	6.5 GeV
Max. Stored Current	60 mA
RF Frequency	508.57 MHz
Circumference	377.26 m
Harmonic Number	640
Number of Bunches	1
Revolution Frequency	795 kHz
Tunes (x/y/s)	10.17/10.23/0.05
Damping Time (x/y/s)	2.5/2.5/1.2 ms
Natural Emittance	294 nm rad
Natural Bunch Length	18.6 mm (62 ps)
Max. Injection Frequency	12.5 Hz
Operation Mode	Decay
Number of Stations	8

* ryota.takai@kek.jp

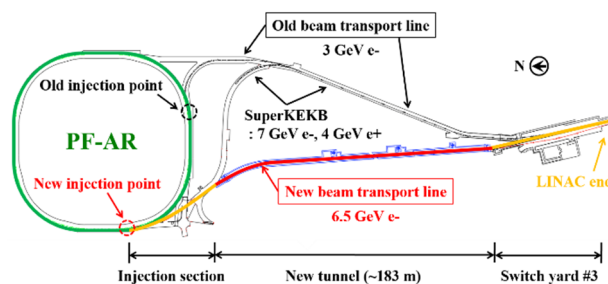


Figure 1: Schematic view of the old and new BTs for PF-AR. The total length of the new BT, from the LINAC end to the new injection point, is about 320 m.

The construction was started in FY2013, followed by the excavation of the new BT tunnel, the development of infrastructure in the tunnel, and the design and production of the required BT components sequentially. The final construction works, such as the deconstruction of the old BT, the relocation of magnets to be reused, the installation of the new BT components, and the reconstruction of the new injection point of PF-AR were proceeded in parallel for seven months from July 2016 to January 2017, and completed on schedule. Following these, the commissioning of the new BT was started and the necessary preparation to resume the user operation could be made in about one month. The new BT is designed for 6.5-GeV full-energy injection and enables not only the simultaneous operation with SuperKEKB but also top-up operations in near future. Besides, it resolves the difficult problems with stacking and accelerating of the 3-GeV short-bunch beam, such as the beam loss due to severe beam instabilities and the heat generation of beam ducts.

In this paper, we describe the beam monitors installed in the new BT for PF-AR in detail and some commissioning results obtained by them.

BEAM MONITORS FOR THE NEW BEAM TRANSPORT LINE OF PF-AR

Figure 1 shows a schematic of the old and new BTs for PF-AR. The new BT is about 320 m long and can be classified into three main sections: Switch Yard #3 for distributing beams to the lower rings at the end of LINAC (SY3), the new BT tunnel dedicated for PF-AR, and the beam injection section connected to the new injection point at the southwestern part of the ring after crossing the existing BT for SuperKEKB. The beam monitors installed in the new BT are listed in Table 2. As the three sections are separated from each other, the control systems of these monitors are arranged sporadically in several local control rooms (LCRs), and the output signals from each monitor are collected through the control network after being digitized at

Content from this work may be used under the terms of the CC BY 3.0 licence (© 2018). Any distribution of this work must maintain attribution to the author(s), title of the work, publisher, and DOI.

the closest LCR (except for GigE cameras for screen monitors that are directly connected to the network). The details of each monitor, listed in Table 2 are as follows.

Table 2: List of PF-AR Beam Monitors

Monitor	Function	Quantity
BPM (Stripline)	Position, Charge	21
SCM (Al ₂ O ₃ :Cr)	Position, Profile	17
BLM (CsI:TI + PMT)	Loss	7
CT	Charge, Timing	2

BPM (Beam Position Monitor)

Twenty-one stripline BPMs are installed in the new BT. Four electrodes are arranged so as to be inscribed in the beam duct of an inner diameter of 52 mm at an angle of 45° around the beam axis. The electrode length is 175 mm except for one BPM, where the electrode length is 125 mm, installed in the upper injection section due to limited installation space. As a result, the frequency, which gives the maximum sensitivity of electrodes becomes approximately an odd multiple of 430 MHz. The electrode thickness is 2 mm, and the width is fixed such that the opening angle relative to the beam axis is 45°. The characteristic impedance of each electrode is designed to be 50 Ω in order to suppress the reflection of beam signals. The electrode end at the lower side is grounded through a common spacer ring. Beam signals induced on the electrode are extracted to the outside through an SMA feedthrough (Kyocera, SMA-R), welded at the upper end of the electrode. The coefficient of the difference-over-sum ratio (an inverse of the position sensitivity coefficient) is 21.0 mm, based on the calculation using CST Particle Studio [3]. The difference-over-sum ratio obtained is approximately proportional to the beam position in the range of -8 to 8 mm from the beam axis. Figure 2 shows a schematic of the BPM head and its photograph after the installation.

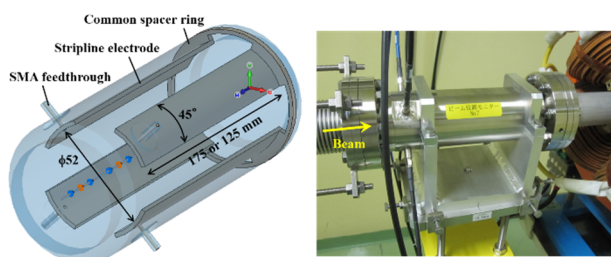


Figure 2: Schematic and photograph of the stripline BPM.

To detect beam signals, we use a log detection circuit originally developed for the compact energy recovery linac (ERL) [4]. The circuit has a band pass filter with a center frequency of 1.3 GHz, a bandwidth of 20 MHz, and a log-linear response to the input power in the range of -90 to -30 dBm, when the front-end attenuator is set to 0 dB. The detected beam signals are digitized by a 12-bit data acquisition unit (Yokogawa, SL1000) and then, the average amplitudes are used in the position calculation. This calculation is performed on the software IOC of the EPICS control system [5]. The transverse positions and charges (the sum

of four output signals) of the injected beams measured by all BPMs are displayed on an orbit monitoring panel and updated synchronously with the beam trigger signals. Figure 3 shows a photograph of the inside of the log detection circuit.

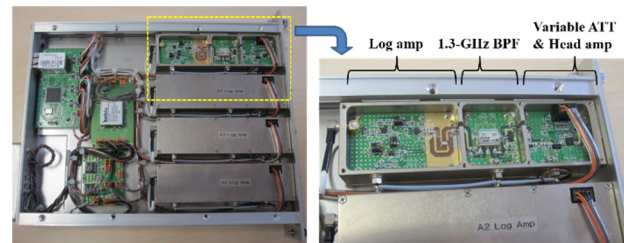


Figure 3: Photograph of the inside of the log detection circuit. The four circuits constitute one NIM module.

SCM (Screen Monitor)

Seventeen SCMs with a scintillating screen are used in the new BT. The internal structure is different between 14 SCMs above the DC septum magnet at the new injection point and the other three SCMs. In the former 14 SCMs, the screen is inserted downward at an angle of 45° to the beam axis and directly observed by a GigE camera (Allied Vision Technologies, Prosilica GC650), which is installed in a cylindrical dark box serving also as a support frame for the SCM duct. In the latter three SCMs, the screen is inserted sideways at an angle of 45° and observed by a camera via a mirror, which are installed in a dark box independent of the support frame. The screen material is a 1-mm-thick alumina scintillator (Desmarquest, AF995R). Four holes of 1-mm-diameter, each located at the peripheral parts of the screen are used for the focus adjustment and the magnification calibration of the imaging optics. A low-distortion CCTV lens with a diaphragm is used with the camera and the magnification is set such that the whole screen area of 30 mm × 30 mm fits within the CCD area. The gain and exposure time of the camera are adjusted carefully to prevent the saturation of the 12-bit CCD pixels. Each camera located around the new injection point, where an especially large amount of beam loss is predicted, is surrounded by a 2-mm-thick lead sheet to protect them from radiation-induced damage. In addition, all of the cameras can be rebooted remotely in case they are frozen due to

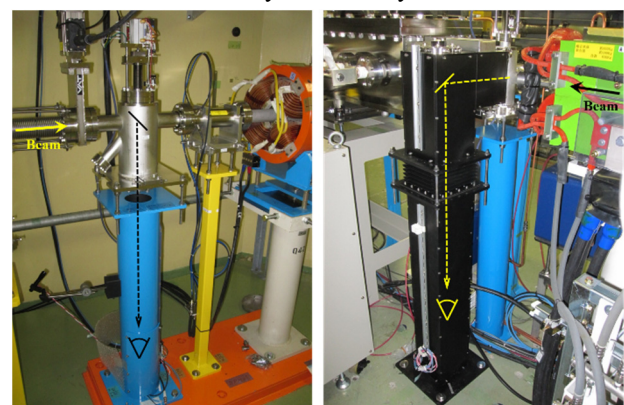


Figure 4: Photographs of the two types of SCMs.

Content from this work may be used under the terms of the CC BY 3.0 licence (© 2018). Any distribution of this work must maintain attribution to the author(s), title of the work, publisher, and DOI.

noise caused by the pulse magnets for beam injection. Figure 4 shows the photographs of the two types of SCMs mentioned above.

The screen image is transferred to IOC for image processing through an Ethernet cable and displayed on each monitoring panel with the results from Gaussian fitting. Synchronizing the screen insertion timing with the start timing of data acquisition can restrict network bandwidth. An automatic measurement program to store the screen image while inserting the screen from the upper side one-by-one, is also provided and used to compare the injected beam profiles with the previous ones. Figure 5 shows a sample of the profile list captured by the automatic program.

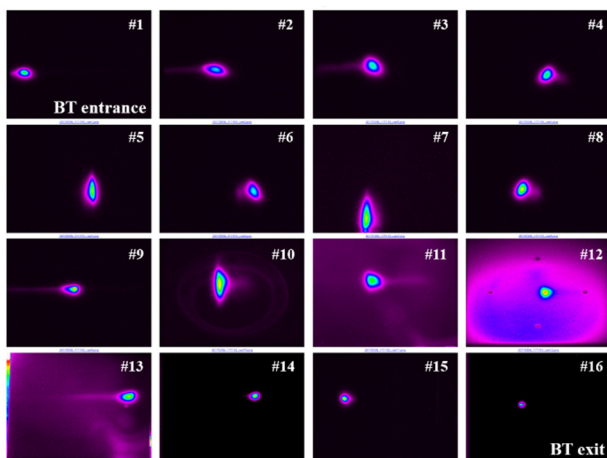


Figure 5: Injected beam profiles along the new BT measured by the SCMs. Data of the last SCM#17 are missing due to an insufficient adjustment of the camera optics.

BLM (Beam Loss Monitor)

Seven BLMs are used to detect radiations caused by the injected beam loss. They are installed at almost equal spacing along the new BT, and used to reduce the local beam loss during injections. At present, they are not included in an interlock system for radiation safety. The detection unit consists of a thallium-doped CsI scintillator and a small photosensor module with a built-in photomultiplier tube and a high voltage power supply (Hamamatsu, H10721). Although the time response of this scintillator is longer than that of a pure CsI scintillator, the sensitivity for the beam loss is higher because of the larger photon

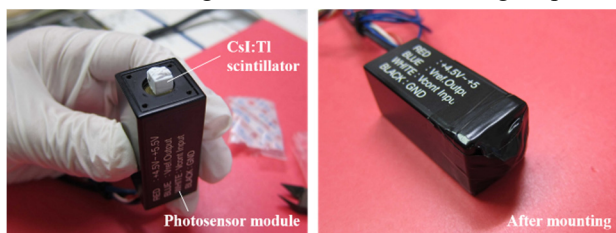


Figure 6: Photographs of the BLM detection unit. The CsI:Tl scintillator is mounted in front of a photoelectric surface of the photosensor module and light-shielded by a black polyester tape.

yield. Furthermore, since this unit is compact and inexpensive, it can be easily installed and extended. Output signals of the BLM are digitized by a general-purpose data acquisition unit similarly to that of the BPM. A power supply and gain of the photosensor module can be remotely controlled through the network. Figure 6 shows photographs of the detection unit.

CT (Current Transformer)

Two CTs are provided at both ends of the new BT, one at each end. The transport efficiency of injected beams can be measured by comparing the area of their output signals. The entrance CT is included in an interlock system to limit the charge of the injected beams, and the exit CT is also used to adjust the timing of the pulse magnets for beam injection. A commercial CT is used, including a ceramic gap to prevent the wall-current flow and a wall-current bypass serving as the RF shield (Bergoz, In-flange ICT). Output signals are processed by a fast oscilloscope or a dedicated circuit attached to the sensor head. Figure 7 shows a photograph of the exit CT.

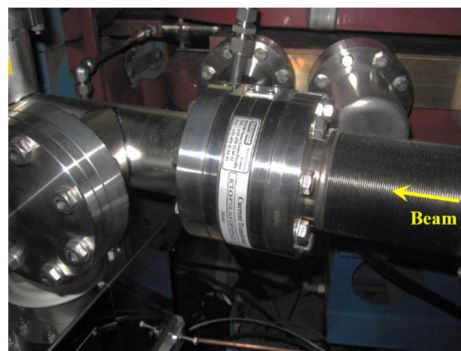


Figure 7: Photograph of the in-flange ICT installed near the exit of the new BT.

COMMISSIONING RESULTS

The beam monitors described in the previous section contributed greatly to accomplish the new BT commissioning in a short period of time. Two experimental results obtained with them during the commissioning are presented here.

The first data is the capture efficiencies of the respective injected beams measured by using the CT. Under the injection frequency of 1 Hz, the change in the capture efficiency during beam injection was investigated by comparing each beam charge with the corresponding increment of the stored current of PF-AR. Although the beam charge was initially supposed to be measured by the entrance CT, the sum of four output signals of a BPM located at the LINAC end, which was calibrated by another CT, was used instead because the entrance CT output was unreliable due to noise from nearby pulse magnets. The transport efficiency of injected beams was almost 100%, confirmed by using the calibrated BPM and the exit CT. The increment of the stored current was measured from the broadband output of a DC current transformer (DCCT) installed in the ring. The result is shown in Fig. 8. The horizontal axis indicates the

identification number of the successively performed measurements, and corresponds to the time of a second unit because of the 1-Hz injection. The left and right vertical axes indicate the capture efficiency of the injected beams and the stored current of the ring, respectively. During this measurement, beam charges injected from LINAC were stable at around 0.24 nC/pulse. The average of the measured capture efficiencies was approximately 85%, whereas it decreased slightly as the stored current increased. In the case of the 5-Hz injection, the averages of the injected beam charges and the capture efficiencies decreased to 0.23 nC/pulse and 83%, respectively. This measurement of the capture efficiency could also be utilized effectively for adjustments of the injection phase and the timing of the pulse magnets for beam injection.

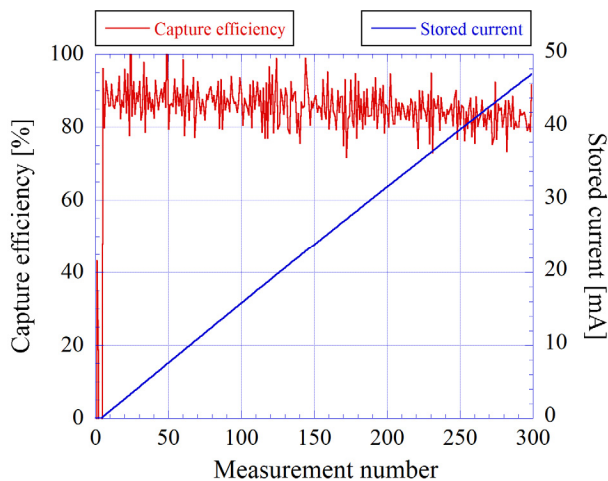


Figure 8: PF-AR capture efficiency measured by using the calibrated BPM and a DCCT for the ring.

The second data is the injected beam loss for every turn measured by using the BLM. As the camera of SCM#15 located between the DC septum magnet and the pulse septum magnet #1 (S1) deteriorated in a shorter period than the other ones, the beam loss was measured by the BLM unit installed under the S1 support frame. The results measured by an oscilloscope are shown in Fig. 9. The horizontal and vertical scales were respectively fixed at 1 μ s/div and 20 mV/div, and it was confirmed in advance that a noise floor due to the stored beam loss was negligibly small. The upper figure is a result with no inserted screens. It can be seen that a portion of the injected beam was lost even under this condition, although only slightly. The lower figure is a result when the screen of SCM#16 located immediately below S1 was inserted, that is, the beam was injected through the screen. The amount of beam loss was increased to about 3 times that in the above condition, and the loss after six turns was also increased. This is because the oscillation of the injected beam grew due to the energy loss at the screen, and it is consistent with the fractional part of the horizontal tune of 0.17. The same BLM unit is planned to be installed around a movable mask located above the RF cavity by the next machine study, and use them to determine the mask length that can prevent the inside of the cavity from being

irradiated by synchrotron radiations without the injected beam loss.

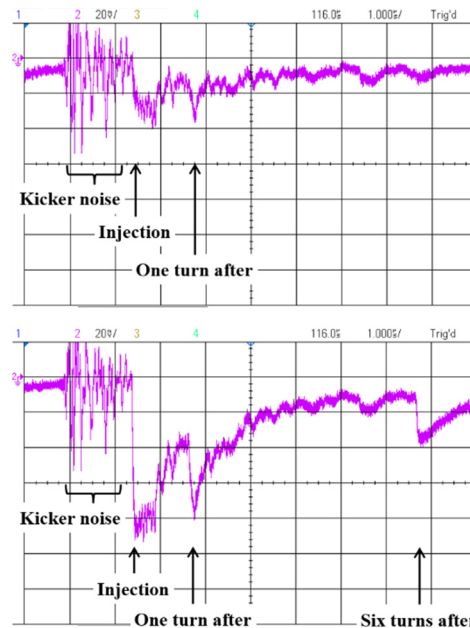


Figure 9: Turn-by-turn measurement of the injected beam loss using the BLM. Without (upper) and with (lower) inserted screens.

Although results are not shown here because they are not beam monitors for the new BT, a turn-by-turn beam position measurement using “Libera Brilliance + [6]”, which is adopted as a BPM circuit for PF-AR, is very useful in the first turn measurement and for the fine adjustment of the kicker timing.

SUMMARY AND FUTURE PLANS

The BT for PF-AR has been recently renewed, such that a full-energy injection can be performed. Standard beam monitors such as BPMs, SCMs, BLMs, and CTs were installed in the new BT, and owing to these the commissioning was completed in one month only. Since April 2017 the user operation without beam acceleration and deceleration has been resumed under full-energy injection. As the next step, we will continue efforts to realize top-up operation. Regarding the beam monitors for the new BT, we are planning the replacement of parts of the BPM circuits with ones with higher resolution, the introduction of high-precision multi-channel ADC boards, and the additional installation of scintillator or optical fiber BLMs.

ACKNOWLEDGEMENTS

The authors would like to thank all the staff of accelerator division VII for their cooperation during the construction and commissioning. We would also like to thank T. Michikawa and Y. Kameta for their support in the development of the control software.

REFERENCES

- [1] N. Higashi *et al.*, “Construction and Commissioning of Direct Beam Transport Line for PF-AR”, in *Proc. IPAC'17*, Copenhagen, Denmark, May 2017, paper WEPAB044, pp. 2678-2680.
- [2] Y. Ohnishi *et al.*, “Dynamic Aperture Optimization in SuperKEKB”, in *Proc. HF2014*, Beijing, China, Oct. 2014, paper FRT1B2, pp. 73-78.
- [3] <https://www.cst.com/products/cstps>
- [4] R. Takai *et al.*, “Design and Initial Commissioning of Beam Diagnostics for the KEK Compact ERL”, in *Proc. IBIC'14*, Monterey, CA, USA, Sep. 2014, paper MOCYB2, pp. 7-11.
- [5] <http://www.aps.anl.gov/epics/>.
- [6] <http://www.i-tech.si/accelerators-instrumentation/libera-brilliance-plus/>.